THE JOURNAL OF PHYSICAL CHEMISTRY Letters

pubs.acs.org/JPCL Letter

Repurposing Low-Molecular-Weight Drugs against the Main Protease of Severe Acute Respiratory Syndrome Coronavirus 2

Jia Gao, Liang Zhang, Xiaodan Liu, Fudong Li, Rongsheng Ma, Zhongliang Zhu, Jiahai Zhang, Jihui Wu, Yunyu Shi, Yueyin Pan, Yushu Ge,* and Ke Ruan*

Cite This: J. Phys. Chem. Lett. 2020, 11, 7267−7272 Read Online

ACCESS | Metrics & More | Article Recommendations | Supporting Information

ABSTRACT: The coronavirus disease pandemic caused by infection with the severe acute respiratory syndrome coronavirus 2 (SARS-CoV-2) has affected the global healthcare system. As low-molecular-weight drugs have high potential to completely match interactions with essential SARS-CoV-2 targets, we propose a strategy to identify such drugs using the fragment-based approach. Herein, using ligand- and protein-observed fragment screening approaches, we identified niacin and hit **1** binding to the catalytic pocket of the main protease (M^{pro}) of SARS-CoV-2, thereby modestly inhibiting the enzymatic activity of M^{pro}. We further searched for low-molecular-weight drugs containing niacin or hit **1** pharmacophores with enhanced inhibiting activity, e.g., carmofur, bendamustine, triclabendazole, emedastine, and omeprazole, in which omeprazole is the only one binding to the C-terminal domain of SARS-CoV-2 M^{pro}. Our study demonstrates that the fragment-based approach is a feasible strategy for identifying low-molecular-weight drugs against the SARS-CoV-2 and other potential targets lacking specific drugs.

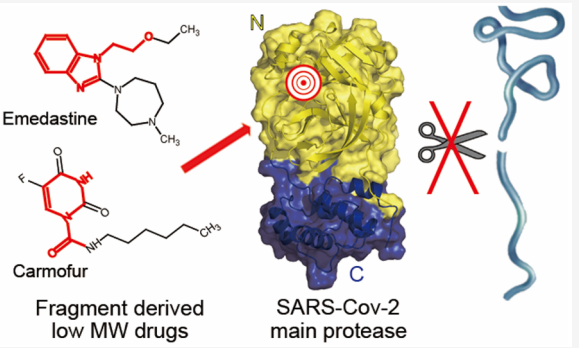

The coronavirus disease (COVID-19) pandemic caused by the severe acute respiratory syndrome coronavirus 2[1−3] (SARS-CoV-2) has so far affected >8 million people worldwide, with a mortality rate over 5%. Main protease (M^{pro} or 3CLpro) is one of the most extensively studied targets of coronaviruses.[4] M^{pro} plays an essential role in the cleavage of viral RNA-translated virus polypeptide[5] and recognizes at least 11 cleavage sites in replicase polyprotein 1ab, e.g., LQ↓SAG (↓ denotes the cleavage site). Covalent inhibitors against the SARS-CoV-2 M^{pro} have recently demonstrated potency toward inhibiting viral replication in cellular assays;[6,7] this further underpins the druggability of M^{pro}. However, these compounds remain in the early stages of preclinical studies, and the development of new drugs usually takes years. The lack of drugs targeting SARS-CoV-2 currently poses a threat to numerous COVID-19 patients.

The COVID-19 pandemic has necessitated the repurposing of oral drugs.[8] As most recently approved drugs have been designed and optimized for specific targets, they are unlikely to completely match interactions with the SARS-CoV-2 targets. Compared with 13 550 potential drugs in the DrugBank database at various stages from preclinical studies through approval, the estimated number of druglike compounds (molecular weight of ∼500 Da) is reportedly approximately 10^{60}. Therefore, the possibility of uncovering a highly potent and specific drug against SARS-CoV-2 is quite slim. Conversely, low-molecular-weight drugs with intermediate potency and high safety can be an alternative treatment against SARS-CoV-2. The toxicity of many low-molecular-weight drugs has been well understood owing to long clinical trials. Furthermore, their low structural complexity increases the odds of fully matching the interactions with anti-SARS-CoV-2 targets; for example, the chemical space of compounds with <11 non-hydrogen atoms is approximately 10^9. This is the cornerstone of fragment-based lead discovery,[9] and many of the compounds in the fragment library were indeed extracted from pharmacophores of approved drugs. We therefore hypothesize that it is highly possible to identify a low-molecular-weight drug containing pharmacophores using fragment-based screening (FBS).

We therefore compared 3508 compounds in our fragment library[10−15] with repurposed drugs from virtual screening, generously released by Prof. Hualiang Jiang at Chinese Academy of Sciences Shanghai Institute of Materia Medica. If these candidates did bind at a high affinity as predicted, their pharmacophores should bind as well, albeit at a weaker affinity. A total of 38 compounds (Table S1) as pharmacophores (substructures) of these repurposed drugs were thus screened

Received: June 18, 2020
Accepted: July 28, 2020
Published: July 28, 2020

https://dx.doi.org/10.1021/acs.jpclett.0c01894
J. Phys. Chem. Lett. 2020, 11, 7267−7272

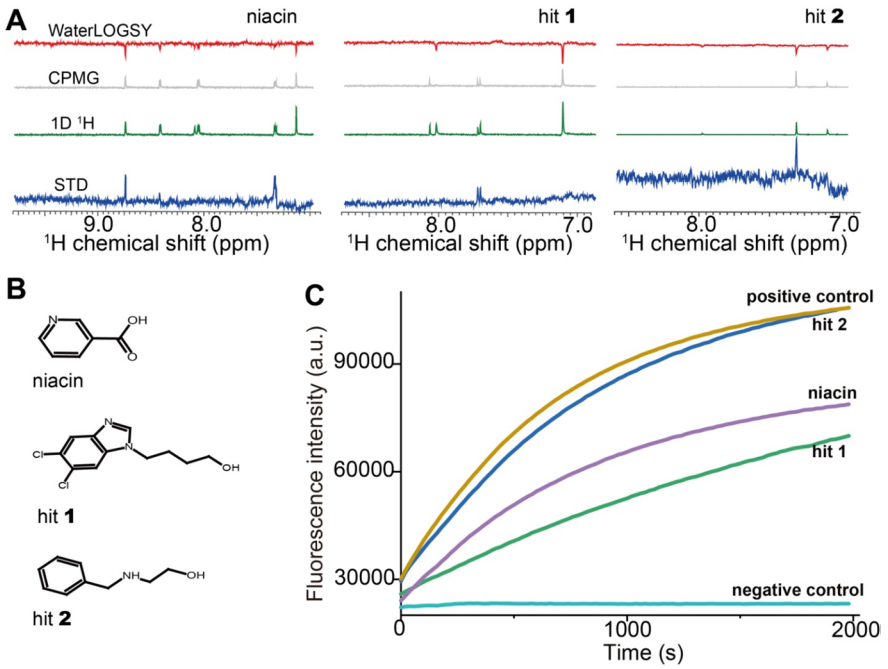

Figure 1. Fragment-based screening identified three hits of the SARS-CoV-2 main protease. (A) NMR ligand-observed spectra of three representative hits in the presence of 10 μM full-length SARS-CoV-2 M^{pro}. (B) Chemical structures of the three hits. (C) Inhibition of the enzymatic activity of the SARS-CoV-2 M^{pro} (5 μM) by the three hits (4 mM). The negative control was treated using fluorescence-labeled peptide (16 μM) in the absence of M^{pro}.

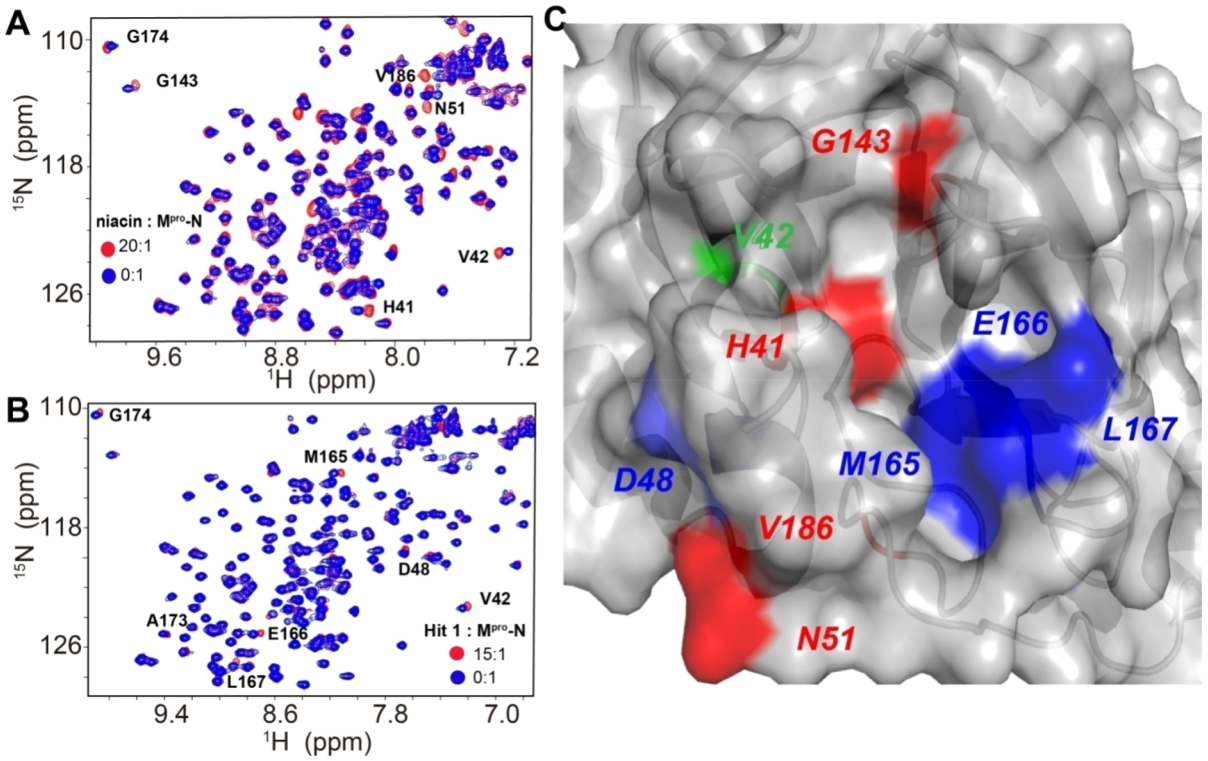

Figure 2. Binding topology of niacin and hit **1** determined from NMR chemical shift perturbations. (A) Superimposition of 2D $^{1}H-^{15}N$ HSQC spectra of the SARS-CoV-2 M^{pro}-N in the absence and presence of niacin. The ligand/protein molar ratios are shown. (B) Chemical shift perturbations induced by hit **1**. (C) Chemical shift perturbations induced by niacin (red), hit **1** (blue), or both (green) were mapped to the surface of the crystal structure of the SARS-CoV-2 M^{pro} (PDB code: 6LU7).

against the SARS-CoV-2 M^{pro} (residue 4-306). These weak binders were readily identified using a nuclear magnetic resonance (NMR) fragment-based approach,[16−18] e.g., the ligand-observed spectra of saturation transfer difference (STD) and WaterLOGSY (Figure 1a). Three hits of the SARS-CoV-2 M^{pro} were identified: niacin, hit **1**, and hit **2** (Figure 1b). The

https://dx.doi.org/10.1021/acs.jpclett.0c01894
J. Phys. Chem. Lett. 2020, 11, 7267−7272

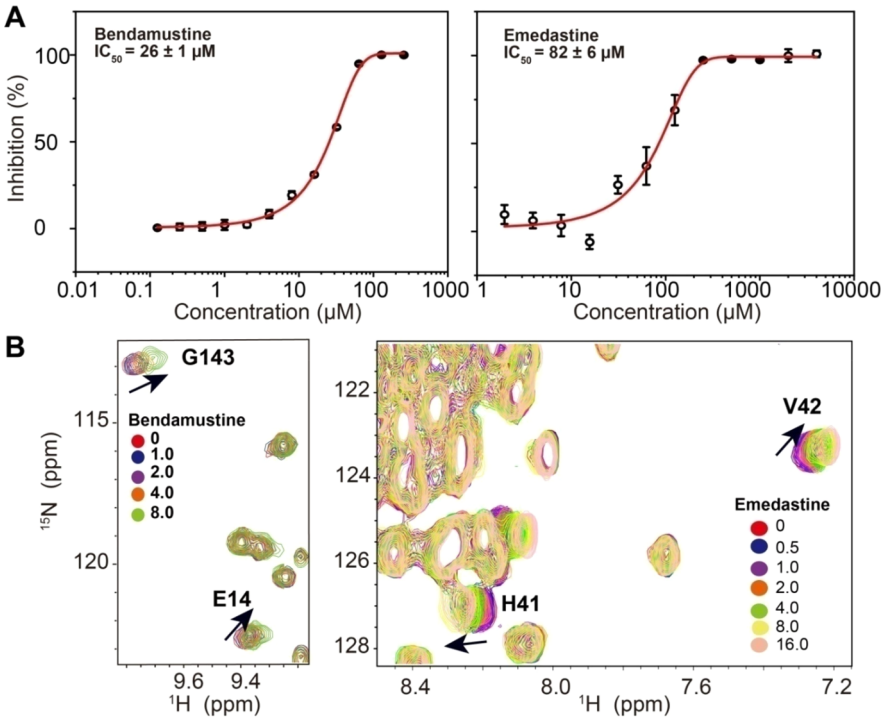

Figure 3. Potency and binding topology of low-molecular-weight drugs as derivatives of hit **1**. (A) Dose-dependent inhibition of the enzymatic activity of the SARS-CoV-2 M^{pro} (0.5 μM) by bendamustine and emedastine in the presence of 16 μM fluorescent-labeled substrate. (B) Chemical shift perturbations of ^{15}N-labeled SARS-CoV-2 M^{pro}-N induced by bendamustine and emedastine at the annotated ligand/protein molar ratio.

hit rate of 8% was slightly higher than that of our FBS against other targets,[19,20] which suggests that the success rate can be enhanced by virtual screening *a priori*. The remaining 35 fragments demonstrated no detectable binding, probably because of the distracting false positives in virtual screening. The potency of the three hits was then evaluated using enzymatic activity assay of the SARS-CoV-2 M^{pro} (Figure 1c). Niacin and hit **1** moderately inhibited the cleavage of fluorescent-labeled polypeptide (FITC-AVLQSGFR-Lys-(Dnp)-Lys-NH2) by the SARS-CoV-2 M^{pro}.

To further map the binding sites of niacin and hit **1**, we determined the chemical shift perturbations (CSPs) of ^{15}N-labeled M^{pro} induced by the titration of these two compounds. However, the severe signal overlap was observed in the heteronuclear single-quantum correlation (HSQC) spectrum of the ^{15}N labeled full-length SARS-CoV-2 M^{pro}. The N-terminus (residues 1-199)[21] and the C-terminus (187-306)[22] of SARS-CoV M^{pro} were separately studied by NMR spectroscopy, and the free-form crystal structures (PDB codes: 2QCY, 4HI3, and 3VB3) reveal remarkable interdomain plasticity of the wild-type or R298A mutant of SARS-CoV M^{pro}.[23−25] Considering the high sequence identity of 96% between the main proteases of SARS-CoV and SARS-CoV-2, the N-terminal domain (M^{pro}-N) with the catalytic core included (residues 4-199) was used with a well-dispersed HSQC spectrum. It thus enabled many ^{1}H−^{15}N amide chemical shift assignments transferred directly from SARS-CoV Mpro-N. Key residues proximal to the catalytic site, including H41, V42, D48, N51, G143, H163, and V186, were thus assigned (Figure S1). Both niacin and hit **1** perturb a common residue V42, suggesting that these two hits bind to the catalytic core of SARS-CoV-2 M^{pro}. Interestingly, these two hits also recognize different sets of residues in the catalytic core; for example, niacin perturbs H41, G143, N51, and V186 (Figure 2a), whereas hit **1** induces CSPs of residues M165, E166, and L167 (Figure 2b). Mapping of these residues to the surface representation of the crystal structure of the SARS-CoV-2 M^{pro} (PDB code: 6LU7)[26] suggested that these two hits adopted different orientations in the catalytic site, with a shared anchor point near V42 (Figure 2c). Considering the molecular size of niacin and the spatial distribution of the perturbed residues, niacin probably binds more than one site. Nevertheless, the CSP pattern suggests that the catalytic core of the SARS-CoV-2 M^{pro} accommodates compounds larger than niacin and hit **1**.

We therefore searched for low-molecular-weight (<400 Da) drugs containing the pharmacophores of niacin and hit **1**. As a niacin derivative, carmofur induced an extra set of cross peaks at a ligand/protein molar ratio of 2:1, and some original signals completely disappeared at a molar ratio of 4:1 (Figure S2a). This indicated a strong binding between carmofur and SARS-CoV-2 M^{pro} as validated by the IC_{50} of 2.8 ± 0.2 μM determined using enzymatic assay at an M^{pro} concentration of 0.5 μM (Figure S2b). However, the original NMR signals of SARS-CoV-2 M^{pro}-N completely disappeared at a ligand/protein molar ratio that significantly deviated from a stoichiometry of 1:1. It has been recently demonstrated that carmofur is a covalent inhibitor of the main protease of the SARS-CoV-2, with an IC_{50} value of 1.82 μM in the presence of 0.2 μM enzyme;[26] this was consistent with our measurement as a higher M^{pro} concentration was used in our case. Collectively, these data suggest that covalent linking to the SARS-CoV-2 M^{pro} is driven by excess carmofur. Nevertheless, using this fragment-based approach is a feasible strategy for repurposing low-molecular-weight drugs targeting SARS-CoV-2 M^{pro}.

Further pharmacophore identification and molecular docking nominated several low-molecular-weight analogues of hit **1**, for example, triclabendazole, emedastine, and bendamustine

https://dx.doi.org/10.1021/acs.jpclett.0c01894
J. Phys. Chem. Lett. 2020, 11, 7267−7272

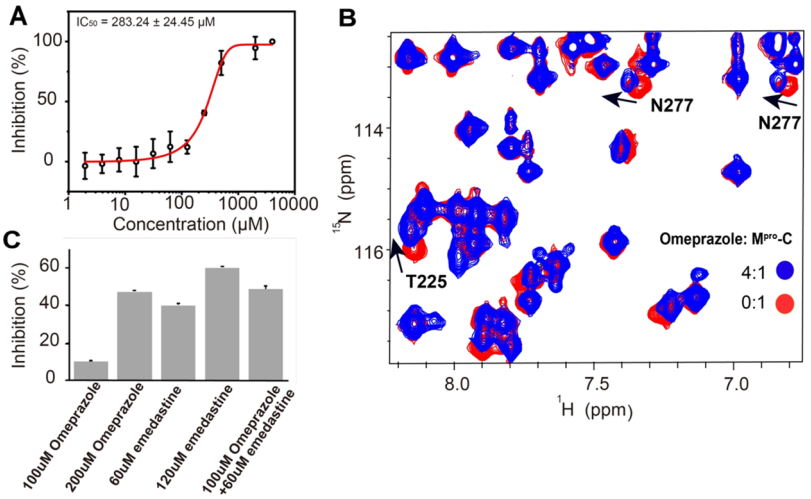

Figure 4. Omprazole suppressed the enzymatic activity via binding to the noncatalytic C-terminus of SARS-CoV-2M^{pro}. (A) Dose-dependent inhibition of the enzymatic activity of the SARS-CoV-2 M^{pro} (0.5 μM) by omeprazole. (B) Chemical shift perturbations of ^{15}N-labeled SARS-CoV-2 M^{pro}-C induced by omeprazoleat the annotated ligand/protein molar ratio. (C) Enzymatic activities of the SARS-CoV-2 M^{pro} (0.5 μM) inhibited by omeprzole or emedastine individually, or by both.

(Figure S3a). The single-dose enzymatic assay showed that these three drugs had significantly higher potency than hit **1** (Figure S3b). We further determined the dose-dependent response of bendamustine and emedastine in the inhibition of the SARS-CoV-2 M^{pro} activity, with IC$_{50}$ values of 26 ± 1 and 82 ± 7 μM (Figure 3a). The IC$_{50}$ value of triclabendazole was roughly estimated to be 70 μM from the two-dose inhibition rates (31% and 72% inhibition at 50 μM and 100 μM triclabendazole, respectively), as limited by the low aqueous solubility of triclabendazole. Further, bendamustine and emedastine induced significantly larger CSPs in a dose-dependent manner than hit **1** (Figure 3b).

In the process of searching for effective low-molecular-weight drugs targeting SARS-CoV-2 M^{pro}, omeprazole as a hit **1** analogue was uncovered capable of inhibiting the protease activity with IC$_{50}$ values of 283 ± 24 μM (Figure 4A). However, omeprazole did not induce any detectable CSPs of the SARS-CoV-2 M^{pro}-N (Figure S4).We hence titrated omeprazole to the ^{15}N-labeled C-terminal protease (M^{pro}-C, residues 187-306) of SARS-CoV-2. Benefiting from the well-dispersed HSQC spectrum of the SARS-CoV-2 M^{pro}-C and high sequence identity with the SARS M^{pro}, we may transfer many ^{1}H−^{15}N amide chemical shift assignments directly (Figure S5)[20]. The omeprazole-induced CSPs (Figure 4B) suggests that omeprazole binds to the C-terminus instead of the catalytic N-terminus of SARS-CoV-2. The docking pose of omeprazole (Figure S6) suggests that it deviates over 17.6 Å from the known N3 covalent inhibitor in the N-terminus of SARS-CoV-2 M^{pro}, which impedes the cross-linking of these two inhibitors. Conversely, omeprazole can be in combinational use with other hit **1** analogues, as the protease activity was mediated by binders in the N- and C-terminus of SARS-CoV-2 M^{pro}. We hence carried out the enzymatic assay of SARS-CoV-2 M^{pro} in the presence of omeprazole or emedastine individually, or both (Figure 4C). The data show that the inhibition of the enzymatic activity of SARS-CoV-2 M^{pro} is additive; that is, cocktails can in principle be used at a lower dose of each component. Thus, less toxicity was expected.

Taken together, our fragment-based strategy facilitates the identification of low-molecular-weight drugs against the SARS-CoV-2 M^{pro}. First, this approach can be readily applied to identify low-molecular-weight drugs against other SARS-CoV-2 targets (e.g., RNA-dependent RNA polymerase or the receptor-binding domain of the spike protein). Second, a combination of these low-molecular-weight drugs may be used to gain higher potency than that achieved via a single compound if their binding topologies show no evidence of steric repulsion. Finally, although carmofur and bendamustine show higher potency than the fragment screening hits, the toxicity of anticancer drugs remains a challenge in their clinical applications. Conversely, triclabendazole, emedastine, or omeprazole could be valuable in inhibiting the SARS-CoV-2 replication at the early stage. These compounds may serve as a new starting point for the next round of drug discovery, as they contain pharmacophores distinct from the published covalent or peptidomimetic inhibitors.[6,7,26−28] In general, our study provides new insights toward the repurposing of low-molecular-weight drugs against the SARS-CoV-2 and other potential targets lacking specific drugs.

■ ASSOCIATED CONTENT

Supporting Information

The Supporting Information is available free of charge at https://pubs.acs.org/doi/10.1021/acs.jpclett.0c01894.

Protein expression and purification, NMR spectroscopy, enzymatic assay of SARS-CoV-2 M^{pro}, and molecular docking (PDF)

■ AUTHOR INFORMATION

Corresponding Authors

Yushu Ge − *Ministry of Education Key Laboratory for Membrane-less Organelles & Cellular Dynamics, Hefei National Laboratory for Physical Sciences at the Microscale, Division of Life Sciences and Medicine, University of Science and Technology of China, Hefei, Anhui 230027, P.R. China*; Email: geyushu@ustc.edu.cn

Ke Ruan − *Ministry of Education Key Laboratory for Membrane-less Organelles & Cellular Dynamics, Hefei National Laboratory for Physical Sciences at the Microscale, Division of Life Sciences and Medicine, University of Science and*

https://dx.doi.org/10.1021/acs.jpclett.0c01894
J. Phys. Chem. Lett. 2020, 11, 7267−7272

Technology of China, Hefei, Anhui 230027, P.R. China; orcid.org/0000-0001-9358-0451; Email: kruan@ustc.edu.cn

Authors

Jia Gao − *Ministry of Education Key Laboratory for Membrane-less Organelles & Cellular Dynamics, Hefei National Laboratory for Physical Sciences at the Microscale, Division of Life Sciences and Medicine, University of Science and Technology of China, Hefei, Anhui 230027, P.R. China*

Liang Zhang − *Ministry of Education Key Laboratory for Membrane-less Organelles & Cellular Dynamics, Hefei National Laboratory for Physical Sciences at the Microscale, Division of Life Sciences and Medicine, University of Science and Technology of China, Hefei, Anhui 230027, P.R. China*

Xiaodan Liu − *Ministry of Education Key Laboratory for Membrane-less Organelles & Cellular Dynamics, Hefei National Laboratory for Physical Sciences at the Microscale, Division of Life Sciences and Medicine, University of Science and Technology of China, Hefei, Anhui 230027, P.R. China*

Fudong Li − *Ministry of Education Key Laboratory for Membrane-less Organelles & Cellular Dynamics, Hefei National Laboratory for Physical Sciences at the Microscale, Division of Life Sciences and Medicine, University of Science and Technology of China, Hefei, Anhui 230027, P.R. China*

Rongsheng Ma − *Ministry of Education Key Laboratory for Membrane-less Organelles & Cellular Dynamics, Hefei National Laboratory for Physical Sciences at the Microscale, Division of Life Sciences and Medicine, University of Science and Technology of China, Hefei, Anhui 230027, P.R. China*

Zhongliang Zhu − *Ministry of Education Key Laboratory for Membrane-less Organelles & Cellular Dynamics, Hefei National Laboratory for Physical Sciences at the Microscale, Division of Life Sciences and Medicine, University of Science and Technology of China, Hefei, Anhui 230027, P.R. China*

Jiahai Zhang − *Ministry of Education Key Laboratory for Membrane-less Organelles & Cellular Dynamics, Hefei National Laboratory for Physical Sciences at the Microscale, Division of Life Sciences and Medicine, University of Science and Technology of China, Hefei, Anhui 230027, P.R. China*

Jihui Wu − *Ministry of Education Key Laboratory for Membrane-less Organelles & Cellular Dynamics, Hefei National Laboratory for Physical Sciences at the Microscale, Division of Life Sciences and Medicine, University of Science and Technology of China, Hefei, Anhui 230027, P.R. China*

Yunyu Shi − *Ministry of Education Key Laboratory for Membrane-less Organelles & Cellular Dynamics, Hefei National Laboratory for Physical Sciences at the Microscale, Division of Life Sciences and Medicine, University of Science and Technology of China, Hefei, Anhui 230027, P.R. China*

Yueyin Pan − *Ministry of Education Key Laboratory for Membrane-less Organelles & Cellular Dynamics, Hefei National Laboratory for Physical Sciences at the Microscale, Division of Life Sciences and Medicine, University of Science and Technology of China, Hefei, Anhui 230027, P.R. China*

Complete contact information is available at: https://pubs.acs.org/10.1021/acs.jpclett.0c01894

Author Contributions

J.G. and Z.L. contributed equally to this work. J.G. and L.Z.: experiment and data analysis. X.L., F.L., R.M., Z.Z., J.Z., J.W., Y.G., and Y.P.: resources. Y.G. and K.R.: conceptualization and writing.

Notes

The authors declare no competing financial interest.

■ ACKNOWLEDGMENTS

Part of our nuclear magnetic resonance study was performed at the National Center for Protein Science Shanghai and the High Magnetic Field Laboratory of the Chinese Academy of Sciences. We thank the Ministry of Science and Technology of China (2019YFA0508400 and 2016YFA0500700), the National Natural Science Foundation of China (21874123, 21703254, and 21807095), the Fundamental Research Funds for the Central Universities (WK2060190086), Hefei National Science Center Pilot Project Funds for the financial support, and we acknowledge supercomputing resources from the Bioinformatics Center of the University of Science and Technology of China, School of Life Sciences.

■ REFERENCES

(1) Chen, N.; Zhou, M.; Dong, X.; Qu, J.; Gong, F.; Han, Y.; Qiu, Y.; Wang, J.; Liu, Y.; Wei, Y.; Xia, J. a.; Yu, T.; Zhang, X.; Zhang, L. Epidemiological and clinical characteristics of 99 cases of 2019 novel coronavirus pneumonia in Wuhan, China: a descriptive study. *Lancet* **2020**, *395* (10223), 507−513.

(2) Li, Q.; Guan, X.; Wu, P.; Wang, X.; Zhou, L.; Tong, Y.; Ren, R.; Leung, K. S. M.; Lau, E. H. Y.; Wong, J. Y.; Xing, X.; Xiang, N.; Wu, Y.; Li, C.; Chen, Q.; Li, D.; Liu, T.; Zhao, J.; Liu, M.; Tu, W.; Chen, C.; Jin, L.; Yang, R.; Wang, Q.; Zhou, S.; Wang, R.; Liu, H.; Luo, Y.; Liu, Y.; Shao, G.; Li, H.; Tao, Z.; Yang, Y.; Deng, Z.; Liu, B.; Ma, Z.; Zhang, Y.; Shi, G.; Lam, T. T. Y.; Wu, J. T.; Gao, G. F.; Cowling, B. J.; Yang, B.; Leung, G. M.; Feng, Z. Early Transmission Dynamics in Wuhan, China, of Novel Coronavirus-Infected Pneumonia. *N. Engl. J. Med.* **2020**, *382* (13), 1199−1207.

(3) Wu, F.; Zhao, S.; Yu, B.; Chen, Y.-M.; Wang, W.; Song, Z.-G.; Hu, Y.; Tao, Z.-W.; Tian, J.-H.; Pei, Y.-Y.; Yuan, M.-L.; Zhang, Y.-L.; Dai, F.-H.; Liu, Y.; Wang, Q.-M.; Zheng, J.-J.; Xu, L.; Holmes, E. C.; Zhang, Y.-Z. A new coronavirus associated with human respiratory disease in China. *Nature* **2020**, *579* (7798), 265−269.

(4) Anand, K.; Ziebuhr, J.; Wadhwani, P.; Mesters, J. R.; Hilgenfeld, R. Coronavirus main proteinase (3CL(pro)) structure: Basis for design of anti-SARS drugs. *Science* **2003**, *300* (5626), 1763−1767.

(5) Hilgenfeld, R. From SARS to MERS: crystallographic studies on coronaviral proteases enable antiviral drug design. *FEBS J.* **2014**, *281* (18), 4085−4096.

(6) Jin, Z.; Zhao, Y.; Sun, Y.; Zhang, B.; Wang, H.; Wu, Y.; Zhu, Y.; Zhu, C.; Hu, T.; Du, X.; Duan, Y.; Yu, J.; Yang, X.; Yang, X.; Yang, K.; Liu, X.; Guddat, L. W.; Xiao, G.; Zhang, L.; Yang, H.; Rao, Z. Structural basis for the inhibition of SARS-CoV-2 main protease by antineoplastic drug carmofur. *Nat. Struct. Mol. Biol.* **2020**, *27* (6), 529−532.

(7) Zhang, L.; Lin, D.; Sun, X.; Curth, U.; Drosten, C.; Sauerhering, L.; Becker, S.; Rox, K.; Hilgenfeld, R. Crystal structure of SARS-CoV-2 main protease provides a basis for design of improved alpha-ketoamide inhibitors. *Science* **2020**, *368* (6489), 409−412.

(8) Li, G.; De Clercq, E. Therapeutic options for the 2019 novel coronavirus (2019-nCoV). *Nat. Rev. Drug Discovery* **2020**, *19* (3), 149−150.

(9) Murray, C. W.; Rees, D. C. The rise of fragment-based drug discovery. *Nat. Chem.* **2009**, *1* (3), 187−192.

(10) Chen, Y. W.; Yiu, C.-P. B.; Wong, K.-Y. Prediction of the SARS-CoV-2 (2019-nCoV) 3C-like protease (3CL pro) structure: virtual screening reveals velpatasvir, ledipasvir, and other drug repurposing candidates. *F1000Research* **2020**, *9*, 129−129.

(11) Kandeel, M.; Al-Nazawi, M. Virtual screening and repurposing of FDA approved drugs against COVID-19 main protease. *Life Sci.* **2020**, *251*, 117627−117627.

(12) Liu, S.; Zheng, Q.; Wang, Z. Potential covalent drugs targeting the main protease of the SARS-CoV-2 coronavirus. *Bioinformatics* **2020**, *36*, 3295.
(13) Ortega, J. T.; Serrano, M. L.; Pujol, F. H.; Rangel, H. R. Unrevealing sequence and structural features of novel coronavirus using in silico approaches: The main protease as molecular target. *EXCLI journal* **2020**, *19*, 400−409.
(14) Ton, A.-T.; Gentile, F.; Hsing, M.; Ban, F.; Cherkasov, A. Rapid Identification of Potential Inhibitors of SARS-CoV-2 Main Protease by Deep Docking of 1.3 Billion Compounds. *Mol. Inf.* **2020**. DOI: 10.1002/minf.202000028
(15) Zhang, D.-h.; Wu, K.-l.; Zhang, X.; Deng, S.-q.; Peng, B. In silico screening of Chinese herbal medicines with the potential to directly inhibit 2019 novel coronavirus. *J. Integr. Med.* **2020**, *18* (2), 152−158.
(16) Liu, J.; Gao, J.; Li, F.; Ma, R.; Wei, Q.; Wang, A.; Wu, J.; Ruan, K. NMR characterization of weak interactions between RhoGDI2 and fragment screening hits. *Biochim. Biophys. Acta, Gen. Subj.* **2017**, *1861* (1), 3061−3070.
(17) Gao, J.; Liang, E.; Ma, R.; Li, F.; Liu, Y.; Liu, J.; Jiang, L.; Li, C.; Dai, H.; Wu, J.; Su, X.; He, W.; Ruan, K. Fluorine Pseudocontact Shifts Used for Characterizing the Protein-Ligand Interaction Mode in the Limit of NMR Intermediate Exchange. *Angew. Chem., Int. Ed.* **2017**, *56* (42), 12982−12986.
(18) Xu, D.; Li, B.; Gao, J.; Liu, Z.; Niu, X.; Nshogoza, G.; Zhang, J.; Wu, J.; Su, X.-C.; He, W.; Ma, R.; Yang, D.; Ruan, K. Ligand Proton Pseudocontact Shifts Determined from Paramagnetic Relaxation Dispersion in the Limit of NMR Intermediate Exchange. *J. Phys. Chem. Lett.* **2018**, *9* (12), 3361−3367.
(19) Nshogoza, G.; Liu, Y.; Gao, J.; Liu, M.; Moududee, S. A.; Ma, R.; Li, F.; Zhang, J.; Wu, J.; Shi, Y.; Ruan, K. NMR Fragment-Based Screening against Tandem RNA Recognition Motifs of TDP-43. *Int. J. Mol. Sci.* **2019**, *20* (13), 3230.
(20) Gao, J.; Ma, R.; Wang, W.; Wang, N.; Sasaki, R.; Snyderman, D.; Wu, J.; Ruan, K. Automated NMR fragment based screening identified a novel interface blocker to the LARG/RhoA complex. *PLoS One* **2014**, *9* (2), No. e88098.
(21) Zhang, S.; Zhong, N.; Ren, X.; Jin, C.; Xia, B. H-1, C-13 and N-15 resonance assignments of SARS-CoV main protease N-terminal domain. *Biomol. NMR Assignments* **2011**, *5* (2), 143−145.
(22) Kang, X.; Zhong, N.; Zou, P.; Zhang, S.; Jin, C.; Xia, B. Foldon unfolding mediates the interconversion between M(pro)-C monomer and 3D domain-swapped dimer. *Proc. Natl. Acad. Sci. U. S. A.* **2012**, *109* (37), 14900−5.
(23) Wu, C. G.; Cheng, S. C.; Chen, S. C.; Li, J. Y.; Fang, Y. H.; Chen, Y. H.; Chou, C. Y. Mechanism for controlling the monomer-dimer conversion of SARS coronavirus main protease. *Acta Crystallogr., Sect. D: Biol. Crystallogr.* **2013**, *69* (5), 747−755.
(24) Chuck, C. P.; Chen, C.; Ke, Z.; Wan, D. C.; Chow, H. F.; Wong, K. B. Design, synthesis and crystallographic analysis of nitrile-based broad-spectrum peptidomimetic inhibitors for coronavirus 3C-like proteases. *Eur. J. Med. Chem.* **2013**, *59*, 1−6.
(25) Shi, J.; Sivaraman, J.; Song, J. Mechanism for controlling the dimer-monomer switch and coupling dimerization to catalysis of the severe acute respiratory syndrome coronavirus 3C-like protease. *J. Virol.* **2008**, *82* (9), 4620−4629.
(26) Jin, Z.; Du, X.; Xu, Y.; Deng, Y.; Liu, M.; Zhao, Y.; Zhang, B.; Li, X.; Zhang, L.; Peng, C.; Duan, Y.; Yu, J.; Wang, L.; Yang, K.; Liu, F.; Jiang, R.; Yang, X.; You, T.; Liu, X.; Yang, X.; Bai, F.; Liu, H.; Liu, X.; Guddat, L. W.; Xu, W.; Xiao, G.; Qin, C.; Shi, Z.; Jiang, H.; Rao, Z.; Yang, H. Structure of Mpro from COVID-19 virus and discovery of its inhibitors. *Nature* **2020**, *582*, 289.
(27) Zhang, L.; Lin, D.; Kusov, Y.; Nian, Y.; Ma, Q.; Wang, J.; von Brunn, A.; Leyssen, P.; Lanko, K.; Neyts, J.; de Wilde, A.; Snijder, E. J.; Liu, H.; Hilgenfeld, R. alpha-Ketoamides as Broad-Spectrum Inhibitors of Coronavirus and Enterovirus Replication: Structure-Based Design, Synthesis, and Activity Assessment. *J. Med. Chem.* **2020**, *63* (9), 4562−4578.
(28) Ma, C.; Sacco, M. D.; Hurst, B.; Townsend, J. A.; Hu, Y.; Szeto, T.; Zhang, X.; Tarbet, B.; Marty, M. T.; Chen, Y.; Wang, J. Boceprevir, GC-376, and calpain inhibitors II, XII inhibit SARS-CoV-2 viral replication by targeting the viral main protease. *Cell Res.* **2020**. DOI: 10.1038/s41422-020-0356-z

https://dx.doi.org/10.1021/acs.jpclett.0c01894
J. Phys. Chem. Lett. 2020, 11, 7267−7272